Synthesis and Characterisation of the First Three-Dimensional Mixed-Metal-Center Inorganic-Organic Hybrid Framework with *N*-(Phosphonomethyl)iminodiacetate

Filipe A. Almeida Paz,[a] Fa-Nian Shi,[b] Jacek Klinowski,[a] João Rocha,*[b] and Tito Trindade[b]

Keywords: Carboxylate ligands / Crystal engineering / Hydrothermal synthesis / N ligands / Organic-inorganic hybrid composites

---

Using crystal engineering concepts, the first three-dimensional (3D) mixed-metal-centre inorganic-organic hybrid frameworks incorporating *N*-(phosphonomethyl)iminodiacetate (pmida^{4-}) were synthesised under mild hydrothermal conditions (100 °C) and characterised structurally. The crystal structures, obtained by the displacement of the coordinated water molecules in $[Co_2V_2O_2(pmida)_2(H_2O)_{10}]\cdot 2(H_2O)$ (**1**) [$P2_1/c$ monoclinic space group, $Z = 2$, $a = 9.996(2)$ Å, $b = 14.854(3)$ Å, $c = 10.781(2)$ Å, $\beta = 110.90(3)°$ and $V = 1495.5(5)$ Å^3] by the rod-like bridging 4,4′-bipyridine (4,4′-bpy) ligand — $[CdVO(pmida)(4,4'\text{-bpy})(H_2O)_2]\cdot(4,4'\text{-bpy})_{0.5}\cdot H_2O$ (**2**) and $[CoVO(pmida)(4,4'\text{-bpy})(H_2O)_2]\cdot(4,4'\text{-bpy})_{0.5}$ (**3**) — are isostructural and were also determined in the $P2_1/c$ monoclinic space group ($Z = 4$) by single-crystal X-ray diffraction studies at low temperature (180 K): for **2**, $a = 9.1267(18)$ Å, $b = 17.610(4)$ Å, $c = 15.361(3)$ Å, $\beta = 93.06(3)°$ and $V = 2465.3(9)$ Å^3; for **3**, $a = 8.7734(18)$ Å, $b = 17.264(4)$ Å, $c = 15.507(3)$ Å, $\beta = 93.94(3)°$ and $V = 2343.2(8)$ Å^3. All the crystal structures contain centrosymmetric dimeric $[V_2O_2(pmida)_2]^{4-}$ units connected to neighbouring M^{2+} cations (Cd^{2+} for **2**, and Co^{2+} for **1** and **3**) through the phosphonate group. In **2** and **3**, extended two-dimensional $[MVO(pmida)(H_2O)_2]_n$ layers are formed, with the 4,4′-bpy molecules acting as pillars between adjacent layers, leading to porous 3D supramolecular structures, $[MVO(pmida)(4,4'\text{-bpy})(H_2O)_2]_\infty$, with a topology resembling that of the NbO net.

Introduction

Since Hoskins and Robson reported the first highly ordered organic-inorganic coordination frameworks,[1] there has been a widespread interest in the design, synthesis and characterisation of such compounds.[2,3] The driving force behind this work is the potential application of functional materials for reversible guest-exchange,[4,5] shape selectivity,[5] catalysis,[6] gas storage,[7] molecular recognition,[8] photoluminescence,[9] and/or unusual magnetic,[10−12] nonlinear[11] and semiconducting properties,[13] chirality[12,14] or clathration.[15] While considerable progress has been made in the understanding of the chemical self-assembly of the building blocks of such materials, reliable prediction of their final topology and chemical properties remains one of the greatest challenges to crystal engineers, since several supramolecular isomers of similar energies are usually formed.[3] However, by careful selection of metallic centres with specific coordination geometries and organic ligands with predictable coordination fashions, some supramolecular motifs can be predicted.

We have focused our research on the synthesis of novel highly crystalline organic-inorganic hybrid materials which incorporate, simultaneously, traditional and novel ligands to the field.[16−18] *N*-(Phosphonomethyl)iminodiacetic acid (H_4pmida) is a precursor of a multidentate organic ligand (pmida^{4-}) with interesting and flexible coordination properties: apart from the two carboxylic acid groups and the central N-donor atom, it contains a phosphonate group capable of coordinating to several metal centres and to eliminate available coordination sites. Surprisingly, searches in the literature and the Cambridge Structural Database produced only a handful of structures incorporating this organic molecule: $Na_4[V_2O_2(pmida)_2]\cdot 10H_2O$ and $Na_8[V_2O_2(pmida)_2]_2\cdot 16H_2O$;[19] $[Co_2(pmida)(H_2O)_5]\cdot H_2O$ and $[Zn_2(pmida)(CH_3CO_2H)]_2\cdot H_2O$;[20] several zirconium derivatives;[21] $\{K_2[CoO_3(pmida)]\}_6\cdot xH_2O$[22] and $[Pb_2(pmida)]\cdot 1.5H_2O$.[23] The structures reported by Crans and co-workers[19] contain a centrosymmetric dimeric $[V_2O_2(pmida)_2]^{4-}$ unit, in which pmida^{4-} completely traps

---

[a] Department of Chemistry, University of Cambridge,
Lensfield Road, Cambridge CB2 1EW, UK
E-mail: jk18@cam.ac.uk
[b] Department of Chemistry, University of Aveiro, CICECO,
3810-193 Aveiro, Portugal
E-mail: rocha@dq.ua.pt

DOI: 10.1002/ejic.200400005

the vanadium centres inside three five-membered rings formed by the two carboxylate groups and the phosphonate group, closely resembling what we have observed for the *N''*-carboxymethyldiethylenetriamine-*N*,*N*,*N'*,*N''*-tetraacetate[17] and nitrilotriacetate[18] ligands. We felt that the $[V_2O_2(pmida)_2]^{4-}$ unit could then be used as a robust building block to construct novel multi-dimensional hybrid materials by replacing the Na^+ counterions with transition metal cations such as Co^{2+} and Cd^{2+}. This was first achieved with Co^{2+} cations which, along with the $[V_2O_2(pmida)_2]^{4-}$ unit, formed centrosymmetric neutral $[Co_2V_2O_2(pmida)_2(H_2O)_{10}]$ species (present in the crystal structure of **1**). Interestingly, each Co^{2+} centre is coordinated to five water molecules, which led us to believe that such weakly bound molecules could be easily displaced by a multitopic rod-like bridging ligand, such as 4,4′-bipyridine (4,4′-bpy). Here, we wish to report the synthesis and structural characterisation of the first two three-dimensional mixed-metallic frameworks incorporating $pmida^{4-}$ and 4,4′-bpy: $[CdVO(pmida)(4,4'\text{-bpy})(H_2O)_2]\cdot(4,4'\text{-bpy})_{0.5}\cdot H_2O$ (**2**) and $[CoVO(pmida)(4,4'\text{-bpy})(H_2O)_2]\cdot(4,4'\text{-bpy})_{0.5}$ (**3**).

Results and Discussion

$[Co_2V_2O_2(pmida)_2(H_2O)_{10}]\cdot 2(H_2O)$ (**1**), $[CdVO(pmida)(4,4'\text{-bpy})(H_2O)_2]\cdot(4,4'\text{-bpy})_{0.5}\cdot H_2O$ (**2**) and $[CoVO(pmida)(4,4'\text{-bpy})(H_2O)_2]\cdot(4,4'\text{-bpy})_{0.5}$ (**3**) were synthesised under mild hydrothermal conditions (see Exp. Sect.) and characterised structurally by single-crystal X-ray diffraction (see Exp. Sect. for further details) [$pmida^{4-}$ = *N*-(phosphonomethyl)iminodiacetate and 4,4′-bpy = 4,4′-bipyridine]. Compounds **2** and **3** have almost identical frameworks, with the most important difference being the extra crystallisation solvent molecule present in **2**. The phase purity and homogeneity of the bulk samples were further confirmed by X-ray powder diffraction analysis and elemental composition studies (EDS and CHN elemental analyses).

All structures contain two crystallographically unique metal centres, M1 and V1 [where M = Co^{2+} (for **1** and **3**) or Cd^{2+} (for **2**)], both in a six-coordination geometry, $\{CoO_6\}$ (in **1**), $\{MO_3N_3\}$ (in **2**/**3**) and $\{VO_5N\}$ [see Figure 1 and (a) in Figure 2; Table 1 and 2]. V1 is always connected to one oxo group and to two $pmida^{4-}$ ligands, with the coordination geometry resembling the typical highly distorted octahedral environment of V^{4+} sites [angles varying from 74.66(8) to 169.94(9)° (for **1**), 75.78(11) to 172.65(13)° (for **2**), and from 75.64(10) to 172.97(12)° (for **3**)], with a short (V=O), four intermediate (V−O) and one long (V−N) bonds (Table 1 and 2), all within the expected ranges reported by Boudin et al.,[24] as found in related compounds. The same authors classify such coordination geometry for V^{4+} as 1+4+1 with, as observed in our struc-

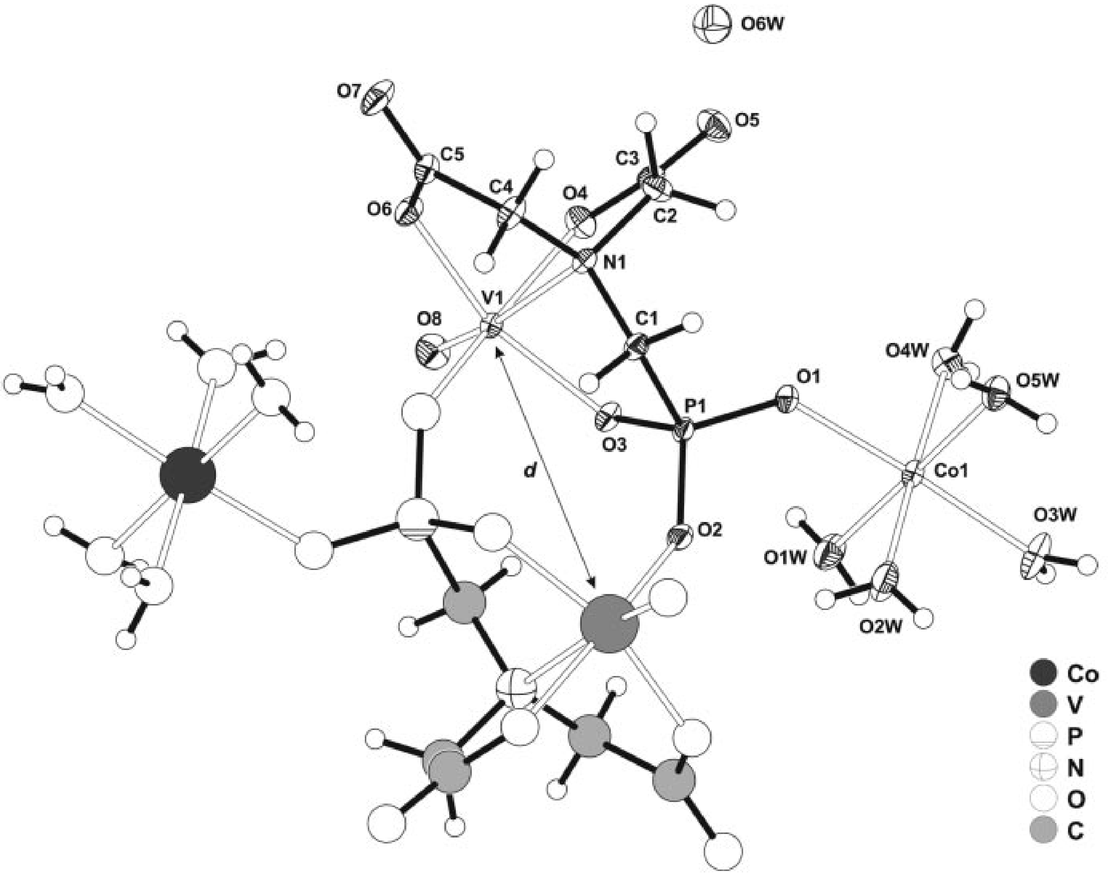

Figure 1. Molecular unit of **1**, showing the labelling scheme for all non-hydrogen atoms belonging to the asymmetric unit [*d* = 5.2285(13) Å]; displacement ellipsoids are drawn at the 50% probability level and H atoms are shown as small spheres; see Table 1 for bond lengths and angles

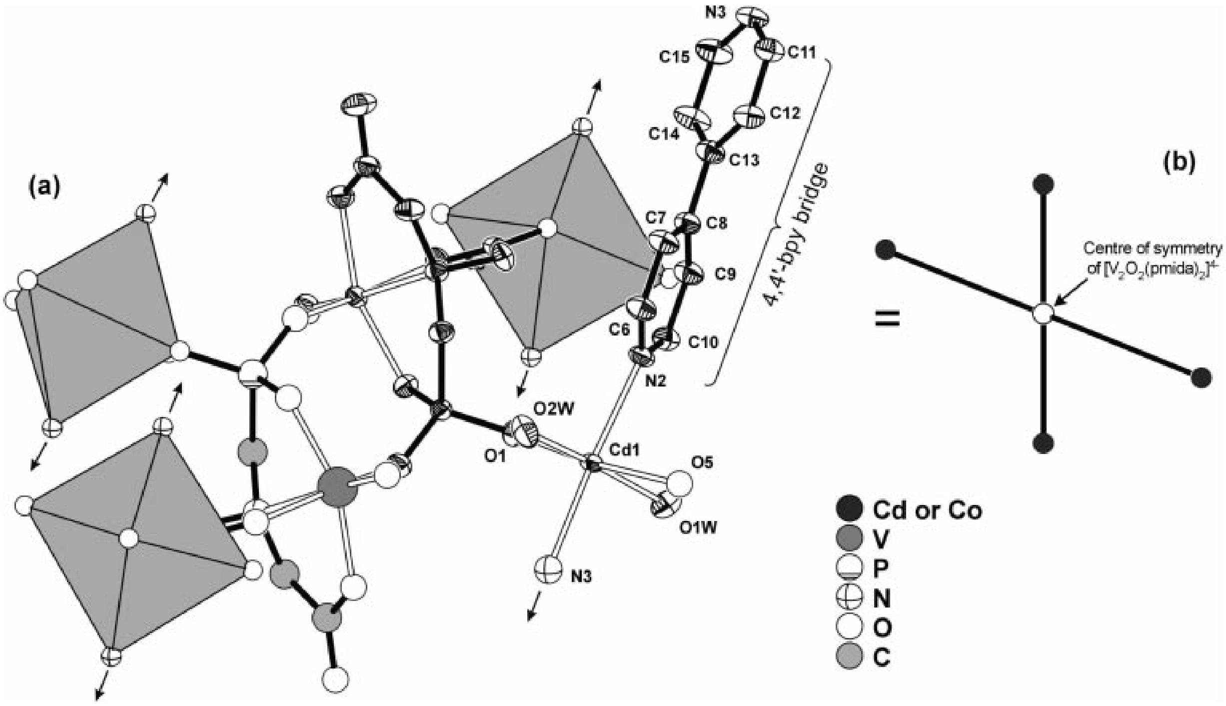

Figure 2. (a) Mixed polyhedral and ball-and-stick, and (b) topological representations of the hexametallic secondary building unit (SBU): section of the [MVO(pmida)(4,4′-bpy)$(H_2O)_2$] framework, showing one $[V_2O_2(pmida)_2]^{4-}$ dimeric unit bridging four $[M(4,4'\text{-bpy})(H_2O)_2]_n^{2n+}$ cationic chains (M = Cd^{2+} and Co^{2+} for **2** and **3**, respectively, represented as grey-filled octahedra); arrows indicate the ditopic bridging 4,4′-bpy ligands; atoms from the asymmetric unit are represented by thermal ellipsoids drawn at the 50% probability level (anisotropic displacement parameters from structure **2**); all hydrogen atoms have been omitted for clarity; see Table 2 for bond lengths and angles

Table 1. Selected bond lengths (Å) and angles (°) for **1**[a]

Co1−O1W	2.095(2)	O3W−Co1−O1W	89.22(9)
Co1−O2W	2.120(2)	O3W−Co1−O2W	87.57(9)
Co1−O3W	2.052(2)	O3W−Co1−O4W	91.57(8)
Co1−O4W	2.139(2)	O3W−Co1−O5W	91.33(8)
Co1−O5W	2.111(2)	O5W−Co1−O2W	88.15(9)
Co1−O1	2.0364(19)	O5W−Co1−O4W	89.81(8)
V1−O2^{i}	1.9897(19)		
V1−O3	1.9957(19)	O2^{i}−V1−O3	91.37(8)
V1−O4	2.0273(19)	O2^{i}−V1−O4	163.89(8)
V1−O6	2.0299(19)	O2^{i}−V1−O6	86.94(8)
V1−O8	1.604(2)	O2^{i}−V1−N1	88.14(8)
V1−N1	2.363(2)	O3−V1−O4	86.80(8)
		O3−V1−O6	154.18(8)
O1−Co1−O1W	88.55(8)	O3−V1−N1	79.54(7)
O1−Co1−O2W	90.52(8)	O4−V1−N1	75.79(8)
O1−Co1−O3W	177.01(9)	O6−V1−O4	87.77(8)
O1−Co1−O4W	90.42(8)	O6−V1−N1	74.66(8)
O1−Co1−O5W	90.91(8)	O8−V1−O2^{i}	101.17(10)
O1W−Co1−O2W	92.31(10)	O8−V1−O3	103.81(10)
O1W−Co1−O4W	89.74(8)	O8−V1−O4	94.81(10)
O1W−Co1−O5W	179.29(8)	O8−V1−O6	101.79(10)
O2W−Co1−O4W	177.77(8)	O8−V1−N1	169.94(9)

[a] Symmetry transformation used to generate equivalent atoms: (i) $2 - x, -y, 1 - z$.

tures, the V=O being *trans* to V−N, showing a marked influence of the oxo ligand in the long V−N distance.[24] Such bonds, although longer than those found in compounds with a *trans* amine nitrogen donor atom bound to vanadium as, for example, complexes with nitrilotriacetic acid (2.17−2.30 Å),[25] *N*-(2-hydroxyethyl)iminodiacetic acid (2.17−2.31 Å),[26] *N*-(carbamoylmethyl)iminodiacetic acid (2.19−2.21 Å),[27] *N*-(carbamoylethyl)iminodiacetic acid (2.17−2.19 Å),[28] (*S*)-[1-(2-pyridyl)ethyl]iminodiacetic acid (2.26−2.29 Å)[29] and triethanolamine (2.15−2.28 Å),[30] are similar to the values found by Crans and co-workers for the vanadium compounds containing pmida^{4-} ligands: {$Na_4[V_2O_2(pmida)_2]\cdot 10H_2O$ (**a**) and $Na_8[V_2O_2(pmida)_2]_2\cdot 16H_2O$ (**b**)}.[19] Since for each compound the four V−O bonds are statistically identical, the coordination geometry for V1 can be seen as a highly distorted octahedral environment (Table 1 and 2).

In **1**, the coordination environment of Co1 is composed of five water molecules and one O-donor atom from the phosphonate group (Figure 1), with a coordination geometry of an almost regular octahedron [bond lengths and angles varying from 2.0364(19) to 2.139(2) Å, and 87.57(9) to 179.29(8)°, respectively] (Table 1). As expected, the bridging rod-like 4,4′-bpy ligand has displaced the weakly bound water molecules, introducing significant structural changes in the final compounds. In **2** and **3**, M1 is now coordinated to six independent moieties (two water molecules, two pmida^{4-} and two 4,4′-bpy ligands) with a coordination geometry of a slightly distorted octahedron [bond angles varying from 84.02(12) to 174.82(1)° (for **2**), and from 86.09(11) to 175.02(9)° (for **3**); see (a) in Figure 2 and Table 2]. Interestingly, each pair of ligand types is *trans*-coordinated in the axial positions, with the O-donor atoms

Table 2. Selected bond lengths (in Å) and angles (in degrees) for **2** and **3**[a]

	2	**3**		**2**	**3**
M1−O1W	2.318(3)	2.117(3)	N2−M1−O2W	94.74(11)	93.40(10)
M1−O2W	2.350(3)	2.128(3)	N2−M1−O5$^{i/iv}$	85.45(11)	86.39(10)
M1−O1	2.252(3)	2.079(2)	N3$^{ii/v}$−M1−O1W	92.14(12)	91.27(10)
M1−O5$^{i/iv}$	2.374(3)	2.218(2)	N3$^{ii/v}$−M1−O2W	84.02(12)	86.09(11)
M1−N2	2.307(3)	2.140(3)	N3$^{ii/v}$−M1−O5$^{i/iv}$	89.42(11)	88.42(10)
M1−N3$^{ii/v}$	2.282(3)	2.129(3)	N3$^{ii/v}$−M1−N2	174.82(12)	174.80(11)
V1−O2$^{iii/vi}$	1.962(3)	1.951(2)			
V1−O3	2.000(3)	2.005(2)	O2$^{iii/vi}$−V1−O3	91.31(11)	91.97(10)
V1−O4	2.032(3)	2.029(2)	O2$^{iii/vi}$−V1−O4	161.34(11)	160.32(10)
V1−O6	2.010(3)	2.026(2)	O2$^{iii/vi}$−V1−O6	88.14(11)	87.41(10)
V1−O8	1.616(3)	1.612(2)	O2$^{iii/vi}$−V1−N1	85.00(11)	84.75(10)
V1−N1	2.341(3)	2.355(3)	O3−V1−O4	88.09(11)	88.20(10)
			O3−V1−O6	153.57(11)	152.36(10)
O1−M1−O1W	91.40(10)	89.59(10)	O3−V1−N1	77.85(11)	76.79(9)
O1−M1−O2W	96.68(10)	95.41(10)	O4−V1−N1	76.64(11)	76.14(9)
O1−M1−O5$^{i/iv}$	174.14(9)	175.02(9)	O6−V1−O4	84.21(12)	83.42(10)
O1−M1−N2	88.81(11)	89.87(10)	O6−V1−N1	75.78(11)	75.64(10)
O1−M1−N3$^{ii/v}$	96.34(11)	95.33(10)	O8−V1−O2$^{iii/vi}$	101.96(13)	101.75(12)
O1W−M1−O2W	171.38(11)	174.54(10)	O8−V1−O3	104.09(13)	105.39(12)
O1W−M1−O5$^{i/iv}$	87.28(10)	87.05(10)	O8−V1−O4	96.26(13)	97.15(12)
O2W−M1−O5$^{i/iv}$	84.98(10)	88.10(10)	O8−V1−O6	101.86(13)	101.77(12)
N2−M1−O1W	88.40(11)	88.80(10)	O8−V1−N1	172.65(13)	172.97(12)

[a] Symmetry transformations used to generate equivalent atoms: (i) x, $1/2 - y$, $1/2 + z$; (ii) $x + 1$, $1/2 - y$, $1/2 + z$; (iii) $2 - x$, $-y$, $1 - z$; (iv) x, $1/2 - y$, $z - 1/2$; (v) $x - 1$, $1 - y$, $z - 1/2$; (vi) $-x$, $-y$, $1 - z$. M = Cd^{2+} or Co^{2+} for **2** and **3**, respectively.

from the two pmida^{4-} ligands being from different functional groups inside this molecule [O1 belongs to the phosphonate group, while O5 belongs to the bridging-η^2-*syn*, *anti*-bidentate C3 carboxylate group; see (a) in Figure 2]. The average M−O and M−N distances are 2.09/2.32/2.14 and 2.29/2.13 Å (for **1**/**2**/**3**), consistent with values found in similar structures.

The pmida^{4-} anion is a polydentate ligand that completely traps the vanadium centres inside three five-membered rings formed by the two carboxylate and phosphonate groups connected in an *anti*-unidentate coordinative fashion to the vanadium centres [pmida-V moiety; Figure 1 and (a) in Figure 2]. The average bite angles are ca. 76.7/76.8/76.2° (for **1**/**2**/**3**, Table 1 and 2), similar to the values for **a** and **b** (ca. 76.7 and 77.0°, respectively).[19] Interestingly, in **2** and **3** each carboxylate group from pmida^{4-} has a different coordination mode: while the C5 group is only coordinated to V1 by the O5 atom in an *anti*-unidentate mode, C3 also forms a bridge with a neighbouring M1 through a bridging-*syn*,*anti*-bidentate coordination mode [V1···Cd1^{i} 5.3463(11) Å, and V1···Co1^{ii} 5.2888(11) Å; symmetry codes: (i) x, $1/2 - y$, $-1/2 + z$; (ii) x, $1/2 - y$, $1/2 + z$]. All carboxylate groups maintain approximately the equivalence in the C−O bonds, with the distances within the 1.239(3)−1.278(3) Å, 1.239(5)−1.277(5) Å and 1.240(4)−1.277(4) Å ranges for structures **1**−**3**, respectively. This is particularly unexpected for the carboxylate groups adopting the *anti*-unidentate coordinative fashion (C5 for all the structures, plus C1 in **1**), and can be explained by the extensive hydrogen-bonding network in the crystal struc-

Table 3. Hydrogen bonding geometry (distances in Å and angles in degrees)[a]

D−H···A	*d*(D−H)	*d*(H···A)	*d*(D···A)	>(DHA)
1				
O1W−H1C···O5^{i}	0.85(1)	1.932(12)	2.770(3)	171(3)
O1W−H1D···O4W^{i}	0.85(1)	2.004(16)	2.817(3)	160(4)
O2W−H2C···O2	0.83(1)	2.13(3)	2.809(3)	139(3)
O2W−H2D···O6W^{ii}	0.84(1)	2.19(4)	2.633(5)	113(4)
O3W−H3A···O6^{iii}	0.84(1)	1.891(12)	2.723(3)	173(4)
O3W−H3B···O4^{i}	0.84(1)	1.902(13)	2.724(3)	166(4)
O4W−H4C···O3^{i}	0.85(1)	1.923(10)	2.769(3)	179(4)
O4W−H4D···O7^{iv}	0.86(1)	1.868(11)	2.719(3)	172(3)
O5W−H5A···O5^{v}	0.84(1)	1.978(14)	2.791(3)	163(3)
O5W−H5B···O7^{iii}	0.84(1)	2.004(12)	2.840(3)	173(3)
O6W···O5	−	−	2.814(5)	−
O6W···O7^{vi}	−	−	2.985(5)	−
2				
O1W−H1C···N4^{vii}	0.86(3)	1.89(4)	2.732(4)	170(5)
O1W−H1D···O4^{viii}	0.86(3)	1.92(4)	2.744(4)	158(6)
O2W−H2C···O8^{ix}	0.85(3)	2.00(3)	2.838(4)	174(4)
O2W−H2D···O7^{i}	0.85(3)	1.86(3)	2.694(4)	167(5)
O3W···O3^{vi}	−	−	2.916(7)	−
O3W···O8^{vi}	−	−	2.898(7)	−
3				
O1W−H1C···N4^{iv}	0.85(3)	1.91(3)	2.740(3)	167(4)
O1W−H1D···O4^{v}	0.84(3)	1.86(3)	2.669(3)	160(5)
O2W−H2C···O8^{x}	0.83(3)	2.04(3)	2.855(4)	169(4)
O2W−H2D···O7^{xi}	0.84(3)	1.85(3)	2.681(4)	175(5)

[a] Symmetry transformations used to generate equivalent atoms: (i) $1 - x$, $-y$, $1 - z$; (ii) x, y, $z - 1$; (iii) $x - 1$, y, $z - 1$; (iv) $x - 1$, $1/2 - y$, $z - 1/2$; (v) x, $1/2 - y$, $z - 1/2$; (vi) $x - 1$, y, z; (vii) $x + 1$, y, z; (viii) x, $1/2 - y$, $1/2 + z$; (ix) $2 - x$, $-y$, $1 - z$; (x) $-x$, $-y$, $1 - z$; (xi) $1 - x$, $-y$, $1 - z$.

tures (Table 3). As in **a** and **b**, the phosphonate group from pmida^{4-} establishes bridges between adjacent vanadium centres (through the O2 and O3 atoms), leading to the formation of a centrosymmetric dimeric unit consisting of two pmida-V moieties, $[V_2O_2(pmida)_2]^{4-}$, and imposing $V1\cdots V1^{iii/iv}$ separations of 5.2285(13)/5.2545(17)/5.2128(16) Å (for **1**/**2**/**3**) [symmetry codes: (iii) 2 − *x*, −*y*, 1 − *z*; (iv) −*x*, −*y*, 1 − *z*; see Figure 1 and (a) in 2].

In the structures reported by Crans and co-workers, the $[V_2O_2(pmida)_2]^{4-}$ dimeric units appear isolated in the crystal structure, interacting only with the neighbouring Na^+ cations and water molecules. Similarly, **1** can be described by the close packing of $[Co_2V_2O_2(pmida)_2(H_2O)_{10}]$ moieties, interacting through the extensive hydrogen-bonding network (not shown; Table 3). However, in **2** and **3** coordinative interactions with Cd^{2+} and Co^{2+} cations from adjacent moieties lead to the formation of extended two-dimensional (2D) $[MVO(pmida)(H_2O)_2]_n$ networks in the *bc* plane of the unit cell (Figure 3). In fact, apart from the bridge created by the C3 *syn*,*anti*-bidentate carboxylate group discussed previously, O1 is also connected to a neighbouring M1 centre, establishing the final tridentate coordination mode for the phosphonate group [$V1\cdots M1$ 6.2903(11)/6.1987(12) Å and $M1\cdots V1^{iii/iv}$ 5.0474(11)/4.9696(11) Å for (**2**/**3**); symmetry codes: (iii) 2 − *x*, −*y*, 1 − *z*; (iv) −*x*, −*y*, 1 − *z*].

As often occurs in other hybrid organic-inorganic materials, **2** and **3** can also be seen as modular structures assembled by the 3D repetition of a discrete hexametallic secondary building unit (SBU) composed of 4 M^{2+} and 2 V^{4+} centres (Figure 2 and 3). Taking the geometrical centres of the $[V_2O_2(pmida)_2]^{4-}$ units (denoted as A) and the M^{2+} metal centres (denoted as X; see Figure 2b and 3b) as network nodes, the $[MVO(pmida)(H_2O)_2]_n$ layers can be seen as undulating plane nets formed by distorted 4-gons assembled by 4- (A) and 2-connected nodes (X) [se (b) in Figure 3]. As expected for a typical AX_2 plane net, A and X are not co-planar, with rows of X-nodes placed above and below the plane of the A-nodes. Such a topological feature has direct consequences in the 3D structure of the compounds. In fact, ditopic bridging 4,4′-bpy molecules [with dihedral angles of ca. 42/44° (**2**/**3**) between the two 4-pyridyl groups; see (a) in Figure 2] establish physical links between consecutive M1 metal centres [see (b) in Figure 2], forming $[M(4,4'\text{-bpy})(H_2O)_2]_n^{2n+}$ cationic chains which run along the crystallographic *a* axis [see (a) in Figure 2 and Figure 4], and act as pillars between consecutive $[MVO(pmida)(H_2O)_2]_n$ layers [$M1\cdots M1^{v}$ 11.613(4)/11.308(4) Å for (**2**/**3**); symmetry code: (v) 1 + *x*, 1/2 − *y*, 1/2 + *z*] (Figure 4).

The parallel stacking of 4,4′-bpy-pillared $[MVO(pmida)(H_2O)_2]_n$ layers leads to a porous 3D supramolecular structure, $[MVO(pmida)(4,4'\text{-bpy})(H_2O)_2]_\infty$ (Figure 4), with a topology resembling that of the NbO net (Figure 5).[31] This 3D structure contains rectangular channels which run along the *a* direction (average cross-section of ca. 5.0 × 4.0 Å^2), and stack in an [ABAB...] brick-wall-like fashion in the *bc* plane (Figure 6). A search for the solvent accessible voids for $[MVO(pmida)(4,4'\text{-bpy})(H_2O)_2]_\infty$ using the software package PLATON[32] (1.20 Å probe radius) gives 596.2/516.9 Å^3 (24.2/22.1% of the total volume of the unit cell) for **2**/**3**. These channels contain the extra crystallisation solvent molecule (in the case of **2**), and 4,4′-bpy molecules strongly hydrogen bonded to the framework, establishing further interactions between consecutive layers (Figure 6 and Table 3).

Thermal Analysis

The course of thermal decomposition of compounds **1**, **2** and **3** is similar. For **1** and **2**, two mass losses in the 54−336 and 30−280 °C temperature ranges, respectively, correspond to the release of all the water molecules from the crystal structure: for **1**, the combined mass losses (24.2%) are in good agreement with the calculated value (23.8%) for the release of the twelve crystallographic water molecules; for **2**, some lattice water is gradually released between 30 and 180 °C (1.4% observed, 2.6% calculated); between 180 and 280 °C all the remaining water molecules are released in a one-step process (7.5% observed, 7.8% calculated).

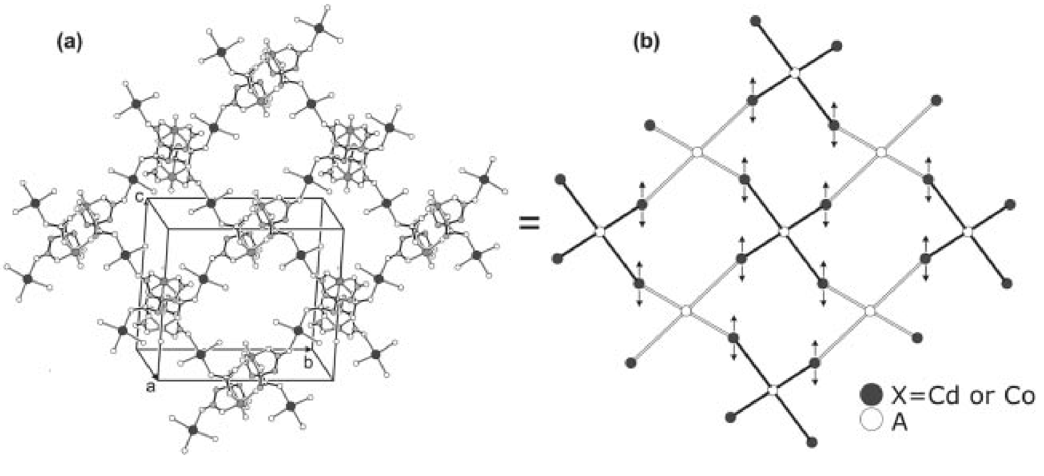

Figure 3. (a) Ball-and-stick and (b) topological representations of 2D $[MVO(pmida)(H_2O)_2]_n$ undulated network; all hydrogen atoms have been omitted for clarity; arrows indicate the ditopic bridging 4,4′-bpy ligands and thus the direction of the $[M(4,4'\text{-bpy})(H_2O)_2]_n^{2n+}$ cationic chains which connect neighbouring $[MVO(pmida)(H_2O)_2]_n$ layers (M = Cd^{2+} and Co^{2+} for **2** and **3**, respectively)

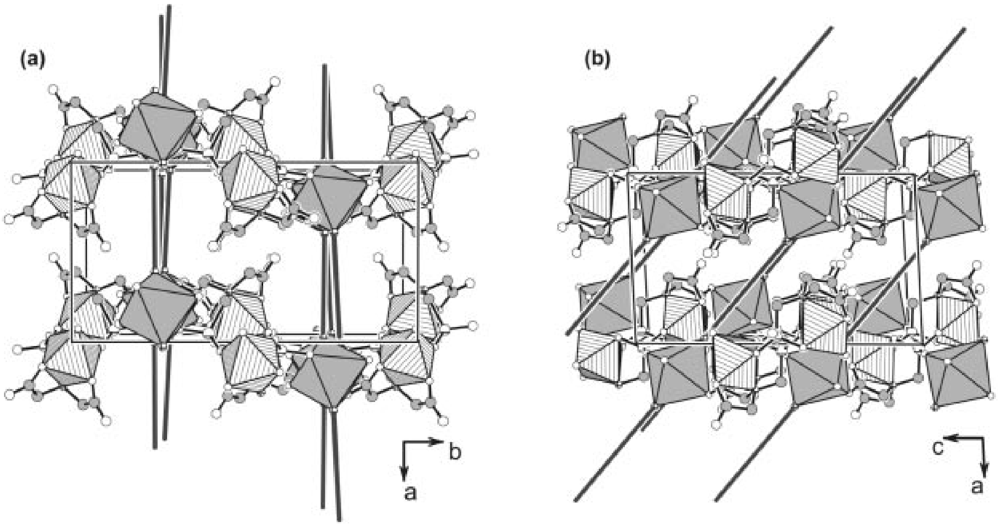

Figure 4. Perspective views along the (a) *c* and (b) *b* crystallographic axes of two consecutive $[MVO(pmida)(H_2O)_2]_n$ layers ($M = Cd^{2+}$ and Co^{2+} for **2** and **3**, respectively), which pack in a parallel fashion along the *a* direction (one layer per *a* axis); the bridging 4,4′-bpy ligands (represented as grey-filled rods) act as pillars between the layers; V^{4+} and M^{2+} centres are represented as white- and grey-filled octahedra, respectively; all hydrogen atoms have been omitted for clarity

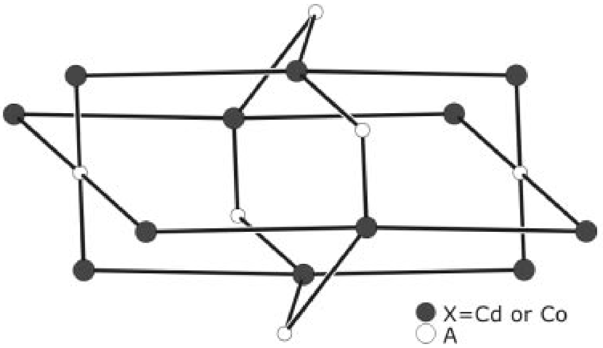

Figure 5. Topological representation of a portion of the $[MVO(pmida)(4,4'\text{-}bpy)(H_2O)_2]_\infty$ network ($M = Cd^{2+}$ and Co^{2+} for **2** and **3**, respectively), showing a topology resembling that of the NbO net[31]

Interestingly, in compound **3** the release of the two molecules per formula unit is significantly faster, with the majority of the water molecules being liberated between 30 and 149 °C (4.9% observed, 5.8% calculated). Although the steric hindrance created by the presence of the 4,4′-bpy molecules within the channels is almost the same for **2** and **3**, the hydrogen bonds caused by the presence of extra lattice water in **2** appear to be responsible for the slow kinetics of the dehydration process (Table 3 and Figure 6).

Up to 606 °C, 520 °C and 655 °C total mass losses of 46.6%, 55.7% and 60.9% are registered for **1**, **2** and **3**, respectively, which is attributed to the thermal decomposition of the organic component, leading to the formation of the mixed oxo-metallic phosphates, MVO_2PO_4 (**1**: 52.1% calculated and 53.4% observed residues; **2**: $M = Cd^{2+}$, 42.2% calculated and 44.3% observed residues; **3**: $M = Co^{2+}$, 38.3% calculated and 39.1% observed residues).

Vibrational Spectra

FT-IR spectroscopy confirms the presence of the organic ligands used in the synthesis (see Exp. Sect.). The presence of hydrogen-bonding networks is evident from the spectra, not only through the presence of the typical O−H stretching vibrations for water molecules (very broad bands), but also to in-plane (δ) and out-of-plane (γ) O−H···O deformations (see Exp. Sect.). The characteristic antisymmetric and symmetric stretching bands for carboxylate ions are also present, with the corresponding $\Delta[\nu_{assym}(CO_2^-) - \nu_{sym}(CO_2^-)]$ values being 218 cm^{-1}, 246 and 189 cm^{-1}, and 250 and 192 cm^{-1} for **1**, **2** and **3**, respectively. These values are a clear indication of the presence of carboxylate groups in the *anti*-unidentate and bridging-η^2-*syn*,*anti*-chelate coordination modes, respectively, as observed in the crystal structures (Figure 1 and 2).[33] The *anti*-unidentate coordination mode for the carboxylate groups is clearly observed in the IR spectra from the typical stretching vibration for C−O groups (found at 1685, 1670 and 1697 cm^{-1} for structures **1**−**3**, respectively).

Conclusion

Crystal Engineering concepts have been used to examine the assembly of ordered 3D solid organic-inorganic hybrid materials containing $[V_2O_2(pmida)_2]^{4-}$ moieties [where $pmida^{4-}$ is *N*-(phosphonomethyl)iminodiacetate]. Two novel isostructural mixed-metal materials containing Cd^{2+} or Co^{2+} have been prepared by using the rod-like 4,4′-bipyridine ligand to establish physical bridges between adjacent $[M_2V_2O_2(pmida)_2]$ moieties. The 3D structures contain pores along the *a* direction of the unit cell that are filled with uncoordinated 4,4′-bipyridine and solvent molecules.

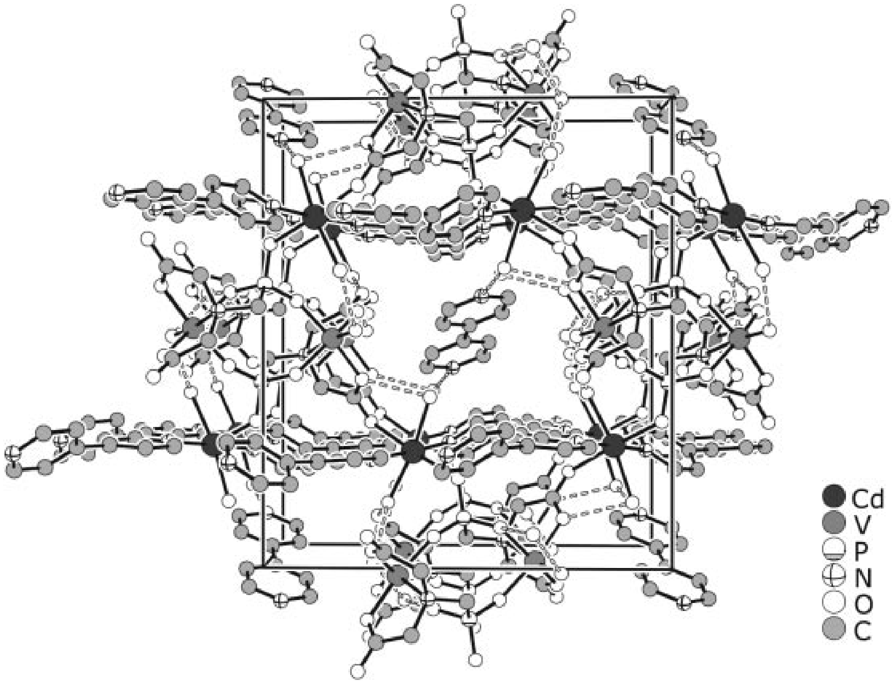

Figure 6. Perspective view along the *a* direction of the unit cell of **2**; hydrogen bonds are represented as white-filled dashed lines (for hydrogen-bonding geometry see Table 3); all hydrogen atoms have been omitted forclarity

Current work is focused on functionalising such materials by selectively controlling the organic pillars and the metal cations bridging adjacent $[V_2O_2(pmida)_2]^{4-}$ moieties.

Experimental Section

General: All reagents were readily available from commercial sources and were used as received without further purification. Syntheses were carried out in PTFE-lined stainless-steel reaction vessels (40 mL) under autogenous pressure and static conditions at 100 °C in a preheated oven. Reactions took place over a period of 4 days after which the vessels were removed from the oven and left to cool to ambient temperature before opening. All compounds proved to be air- and light-stable, and insoluble in water and common organic solvents such as methanol, ethanol, acetone, dichloromethane, toluene, DMSO and chloroform.

Characterisation: Elemental analyses for C, H and N were performed on an Exeter Analytical CE-440 Elemental Analyzer (University of Cambridge). Samples were combusted under oxygen at 975 °C, with He as the purge gas. FT-IR spectra were measured from KBr disks (Aldrich, 99%+, FT-IR grade) on a Matson 700 FTIR spectrometer. Thermogravimetric analyses (TGA) were carried out using a Shimadzu TGA-50, with a heating rate of 10 °C/min, under nitrogen atmosphere with flow rate of 20 mL/min.

Preparation and Structural Characterisation of $[CoVO(pmida)(H_2O)_5]_2 \cdot 2(H_2O)$ (1): A mixture of vanadium(IV) oxide sulfate pentahydrate ($VOSO_4 \cdot 5H_2O$; 0.40 g, 99% Sigma-Aldrich), cobalt acetate tetrahydrate ($CoC_4H_6O_4 \cdot 4H_2O$; 0.620 g, 99.0% Fluka), *N*-(phosphonomethyl)iminodiacetic acid hydrate (H_4pmida; 0.400 g, 97% Fluka), and imidazole ($C_3H_4N_2$; 0.200 g, 99.0% Panreac) in about 8 mL of distilled water, was stirred thoroughly for 30 min at ambient temperature yielding a suspension with a molar composition of 1.00:1.56:1.19:1.86:281, respectively. After the reaction a large amount of big purple crystals of **1** (ca. 0.50 g) were isolated by vacuum filtering, washed with large amounts of distilled water (3 × ca. 50 mL), and air-dried at ambient temperature. Large single-crystals of **1** could also be formed by the slow evaporation of water from the autoclave mother liquor. $C_{10}H_{32}Co_2N_2O_{28}P_2V_2$ (910.06) (based on single-crystal data): calcd. C 13.14, H 3.97, N 3.06; found C 13.63, H 3.72, N 2.89. TGA data (mass losses): 54−169 °C 18.8% (DTG peak at 142 °C); 169−336 °C 5.4% (DTG peak at 171 °C); 336−440 °C 20.4% (DTG peaks at 379 and 403 °C); 440−606 °C 2.0% (DTG peak at 501 °C). Selected FT-IR data (cm^{-1}): ν(O−H, lattice and coordinated water) = 3384 vs (very broad); ν_{sym}(C−H in CH_2) = 2962 m; ν_{asym}(C−H in CH_2) = 2925 m; ν(C−O) = 1695 m; $\nu_{asym}(CO_2^-)$ = 1622 vs; $\delta(CH_2)$ = 1427 m; $\nu_{sym}(CO_2^-)$ = 1404 s; δ(O−H···O) = 1389 s and 1343 m; ν(C−O) = 1254 m; δ(C−C−N, amines) = 1145 vs and 1116 s; ν(N−C) = 1103s; ν(P−O) = 1061 vs; ν(V−O) = 955 s; γ(O−H···O) = 909 m; ν(P−C) = 774 m; γ(C−O) = 737 m.

Preparation and Structural Characterisation of $[CdVO(pmida)(4,4'\text{-bpy})(H_2O)_2] \cdot (4,4'\text{-bpy})_{0.5} \cdot H_2O$ (2): A mixture of vanadium(IV) oxide sulfate pentahydrate ($VOSO_4 \cdot 5H_2O$; 0.40 g, 99% Sigma−Aldrich), cadmium oxide (CdO; 0.470 g, 99% Fluka), *N*-(phosphonomethyl)iminodiacetic acid hydrate (H_4pmida; 0.560 g, 97% Fluka) and 4,4′-bipyridine (4,4′-bpy; 0.190 g, 99% Fluka) in about 15 mL of distilled water, was stirred thoroughly for 30 min at ambient temperature yielding a suspension with a molar composition of 1.30:2.77:2.04:1.00:685, respectively. After the reaction the resulting mixture consisted of two distinct phases: a large amount of light-blue crystals of **1** (ca. 0.20 g), and a residual amount of a white powder of unknown composition. The two components were readily separated by vacuum filtering and washing with large amounts of distilled water (3 × ca. 50 mL). Crystals of **2** were manually harvested and then air-dried at 70 °C. $C_{20}H_{22}CdN_4O_{11}PV$ (688.73) (based on single-crystal data): calcd. C 34.78, H 3.50, N 8.11; found C 33.72, H 3.32, N 7.72. TGA data (mass losses): 30−180 °C 1.4% (DTG peak at 50 °C); 180−280 °C 6.1% (DTG peak at 216 °C);

280−520 °C 48.2% (DTG peaks at 366 °C and 430 °C). Selected FT-IR data (cm^{-1}): ν(O−H, lattice and coordinated water) = 3381 vs (very broad); 3140 vs (very broad); ν(C−H, aromatic compounds) = 3055 s; 3036 s; ν_{sym}(C−H in CH_2) = 2963 m; ν_{asym}(C−H in CH_2) = 2917 m; overtones and combination bands for 4-monosubstituted pyridines = 1966 w and 1940 w; ν(C−O) = 1670 sh; ν_{asym}(CO_2^-) = 1632 vs and 1601 vs; interactions between ν(C−C) and ν(C−N) for 4-monosubstituted pyridines = 1565 m and 1489 m; ν(C−H, aromatic compounds) = 1535 m; δ(CH_2) = 1428 m; ν_{sym}(CO_2^-) = 1412 s and 1386 s; δ(O−H···O) = 1343 m and 1325 m; ν(C−O) = 1266 m and 1254 m; δ(C−H, 4-monosubstituted pyridines) = 1219 m and 1099 s; ρ(C−H) = 1160 s and 1050 s; δ(C−C−N, amines) = 1123 s and 1113 s; ν(N−C) = 1098 vs and 1075 vs; ν(P−O) = 1050 vs; interactions between ν(C−C) and ν(C−N) for 4-monosubstituted pyridines = 992 m; ν(V−O) = 946 s; γ(O−H···O) = 911 m; γ(=C−H, 4-monosubstituted pyridines) = 855 m and 805 s; ν(P−C) = 783 vs; γ(C−O) = 732 m; δ(C−N−C, tertiary amines) = 556 m (very broad); ρ[(C−O)−O] 490 m and 514 m.

Preparation and Structural Characterisation of [CoVO(pmida)(4,4′-bpy)(H_2O)$_2$]·(4,4′-bpy)$_{0.5}$ (3): A mixture of vanadium(IV) oxide sulfate pentahydrate ($VOSO_4·5H_2O$; 0.40 g, 99% Sigma−Aldrich), cobalt acetate tetrahydrate ($CoC_4H_6O_4·4H_2O$; 0.310 g, 99.0% Fluka), *N*-(phosphonomethyl)iminodiacetic acid hydrate (H_4pida; 0.280 g, 97% Fluka), 4,4′-bipyridine (4,4′-bpy; 0.100 g, 99% Fluka), and sodium hydroxide (NaOH; 0.20 g, 98.0% Panreac) in ca. 10 g of distilled water, was stirred thoroughly for 30 min at ambient temperature yielding a suspension with a molar composition of 2.47:1.94:1.94:1.00:7.81:867, respectively. After the reaction the resulting mixture consisted of three distinct phases: a large amount of big purple-pink crystals of **2** (ca. 0.21 g), and a residual amount of small mixed particles of unknown microcrystalline compounds. These components were readily separated by vacuum filtering and washing with large amounts of distilled water (3 × ca. 50 mL). Crystals of **3** were manually harvested and air-dried at ambient temperature. $C_{20}H_{22}CoN_4O_{10}PV$ (619.26) (based on single-crystal data): calcd. C 38.79, H 3.58, N 9.05; found C 38.23, H 3.56, N 8.83. TGA data (mass losses): 30−149 °C 4.9% (DTG peak at 119 °C); 215−265 °C 4.7% (DTG peak at 250 °C); 265−335 °C 18.3% (DTG peak at 301 °C); 335−366 °C 10.5% (DTG peak at 343 °C); 366−478 °C 8.0% (DTG peaks at 377 and 400 °C); 478−655 °C 14.5% (broad DTG peak at 575 °C). Selected FT-IR data (cm^{-1}): ν(O−H, lattice and coordinated water) = 3395 vs (very broad); ν(C−H, aromatic compounds) = 3063 s; 3044 s; ν_{sym}(C−H in CH_2) = 2962 m and 2953 m; ν_{asym}(C−H in CH_2) = 2923 m and 2912 m; ν(C−O) = 1697 m; ν_{asym}(CO_2^-) = 1651 vs and 1610 vs; interactions between ν(C−C) and ν(C−N) for 4-monosubstituted pyridines = 1578 m and 1491 m; ν(C−H, aromatic compounds) = 1536 m; δ(CH_2) = 1428 m; ν_{sym}(CO_2^-) = 1418 s and 1401 s; δ(O−H···O) = 1358 m and 1336 m; ν(C−O) = 1261 m and 1249 m; δ(C−H, 4-monosubstituted pyridines) = 1221 m and 1205 m; δ(C−C−N, amines) = 1128 s and 1117 s; ν(N−C) = 1103 vs and 1095 vs; ν(P−O) = 1062 vs and 1049 s; ν(V−O) = 949 s; γ(O−H···O) = 910 m; γ(=C−H, 4-monosubstituted pyridines) = 862 m, 821 vs, 800 s; ν(P−C) = 787 m; γ(C−O) = 733 m; δ(ring, 4-monosubstituted pyridines) = 635 s.

X-ray Crystallographic Studies: Suitable single crystals of [$Co_2V_2O_2$(pmida)$_2$(H_2O)$_{10}$]·2(H_2O) (**1**), [CdVO(pmida)(4,4′-bpy)(H_2O)$_2$]·(4,4′-bpy)$_{0.5}$·H_2O (**2**) and [CoVO(pmida)(4,4′-bpy)(H_2O)$_2$]·(4,4′-bpy)$_{0.5}$ (**3**) were mounted on a glass fibre using perfluoropolyether oil.[34] Data were collected at 180(2) K on a Nonius−Kappa charge-coupled device (CCD) area-detector diffractometer (Mo-K_α graphite-monochromated radiation, λ = 0.7107 Å), equipped with an Oxford Cryosystems cryostream and controlled by the Collect software package.[35] Images were processed with Denzo and Scalepack,[36] and the data were corrected for absorption by using the empirical method employed in Sortav.[37] Structures were solved by the direct methods of SHELXS-97,[38] and refined by full-matrix least-squares on F^2 using SHELXL-97.[39] All non-hydrogen atoms were directly located from difference Fourier maps and refined with anisotropic displacement parameters.

In **2** and **3**, the crystallographically unique 4-pyridyl group from the uncoordinated 4,4′-bpy molecule was found to be affected by thermal disorder, with the last difference Fourier map syntheses showing a large residual electron density around the aromatic ring: for **2**, the highest peak (2.661 e·Å^{-3}) was located at 0.67 Å from C17, and the deepest hole (−2.660 e·Å^{-3}) at 0.17 Å from C16; for **3**, the highest peak (1.737 e·Å^{-3}) was located at 0.57 Å from C16, and the deepest hole (−1.079 e·Å^{-3}) at 0.46 Å from C16. In **2**, only N4 was satisfactorily refined using anisotropic treatment, with all the carbon atoms receiving a single common isotropic displacement parameter; in **3**, atoms from the uncoordinated 4-pyridyl group were generally refined using an anisotropic treatment, with the exception of C16 and C17, for which a common isotropic displacement parameter was used instead. AFIX 66 instruction was also applied in the earlier stages of the refinement in order to ensure a reasonable geometry for the uncoordinated 4-pyridyl aromatic rings.

The hydrogen atoms attached to carbon were located at their idealised positions, and included in the refinement in a riding-motion approximation with an isotropic thermal displacement parameter fixed at 1.2-times U_{eq} of the atom to which they are attached. Hydrogen atoms from coordinated water molecules were directly located from difference Fourier maps and refined using independent isotropic displacement parameters. The O−H and H···H distances were restrained to 0.84(2) and 1.37 Å, respectively, to ensure a chemically reasonable geometry for the water molecules. These O−H bonds are intended to provide the best fit for the X-ray data, but they do not reflect the true position of the hydrogen nucleus. For **1** and **2**, the crystallisation water molecules were also directly located from difference Fourier maps. Although in **1** the O-atom could be successfully refined using anisotropic thermal displacement parameters, in **2** such treatment gave large tensors in more than one direction, suggesting that the atom is affected by thermal disorder (the atom was instead refined with isotropic thermal displacement parameters). No attempt was made to place the hydrogens on these oxygen atoms and, consequently, the empirical formulae are four and two H atoms short per formula unit, for **1** and **2**, respectively.

All cavity dimensions were calculated by overlapping rigid spheres with van der Waals radii for each element: O 1.52 Å, N 1.55 Å, C 1.7 Å, Cd 2.2 Å, Co 2.0 Å, V 2.0 Å and P 1.8 Å (hydrogen atoms were omitted in all cases for simplicity). Information concerning crystallographic data collection and structure refinement for structures **1** to **3** is summarised in Table 4. Selected bond lengths and angles are given in Table 1 (for **1**) and 2 (for **2** and **3**), and hydrogen-bonding geometry in Table 3.

CCDC-220439 (for **1**), -214332 (for **2**) and -219881 (for **3**) contain the supplementary crystallographic data for this paper. These data can be obtained free of charge at www.ccdc.cam.ac.uk/conts/retrieving.html [or from the Cambridge Crystallographic Data Centre, 12 Union Road, Cambridge CB2 1EZ, UK; Fax: +44 1223 336 033; E-mail: deposit@ccdc.cam.ac.uk].

Table 4. Crystal data and structure refinement information for **1−3**

	1[a]	**2**[a]	**3**
Formula	$C_{10}H_{32}Co_2N_2O_{28}P_2V_2$	$C_{20}H_{22}CdN_4O_{11}PV$	$C_{20}H_{22}CoN_4O_{10}PV$
Molecular mass	910.06	688.73	619.26
Crystal system	monoclinic	monoclinic	monoclinic
Space group	$P2_1/c$	$P2_1/c$	$P2_1/c$
a (Å)	9.996(2)	9.1267(18)	8.7734(18)
b (Å)	14.854(3)	17.610(4)	17.264(4)
c (Å)	10.781(2)	15.361(3)	15.507(3)
β (°)	110.90(3)	93.06(3)	93.94(3)
Volume (Å^3)	1495.5(5)	2465.3(9)	2343.2(8)
Z	2	4	4
D_c (g cm^{-3})	2.021	1.856	1.755
μ(Mo-K_α) (mm^{-1})	1.916	1.374	1.241
F(000)	920	1376	1260
Crystal size (mm)	0.23 × 0.18 × 0.16	0.32 × 0.28 × 0.23	0.12 × 0.10 × 0.07
Crystal type	purple blocks	green blocks	purple blocks
θ range	3.73 to 27.47	3.52 to 27.47	3.54 to 27.48
Index ranges	$-12 \le h \le 12$	$-11 \le h \le 11$	$-11 \le h \le 11$
	$-19 \le k \le 19$	$-22 \le k \le 22$	$-22 \le k \le 22$
	$-13 \le l \le 13$	$-19 \le l \le 19$	$-20 \le l \le 20$
Reflections collected	8406	14579	19973
Independent reflections	3400 (R_{int} = 0.0243)	5600 (R_{int} = 0.0296)	5336 (R_{int} = 0.0562)
Final *R* indices [$I > 2\sigma(I)$]	$R1 = 0.0332$	$R1 = 0.0455$	$R1 = 0.0491$
	$wR2 = 0.0369$	$wR2 = 0.1139$	$wR2 = 0.1100$
Final *R* indices	$R1 = 0.1011$	$R1 = 0.0494$	$R1 = 0.0701$
(all data)	$wR2 = 0.1040$	$wR2 = 0.1174$	$wR2 = 0.1204$
Largest diff. peak and hole	0.562 and −0.924 e·Å^{-3}	2.661 and −2.660 e·Å^{-3}	1.737 and −1.079 e·Å^{-3}

[a] Empirical formula is four (for **1**) and two (for **2**) H atoms short.

Acknowledgments

We are grateful to FEDER, POCTI (Portugal), and to the Portuguese Foundation for Science and Technology (FCT) for their general financial support and also the Ph.D. and Post-Doctoral research grants Nos. SFRH/BD/3024/2000 (to F. A. A. P.) and SFRH/BPD/9309/2002 (to F.-N. S.).

---

[1] B. F. Hoskins, R. Robson, *J. Am. Chem. Soc.* **1990**, *112*, 1546−1554.

[2] S. R. Batten, R. Robson, *Angew. Chem. Int. Ed.* **1998**, *37*, 1461−1494; S. Kitagawa, M. Kondo, *Bull. Chem. Soc. Jpn.* **1998**, *71*, 1739−1753; M. J. Zaworotko, *Chem. Commun.* **2001**, 1−9; P. J. Hagrman, D. Hagrman, J. Zubieta, *Angew. Chem. Int. Ed.* **1999**, *38*, 2639−2684; O. M. Yaghi, H. L. Li, C. Davis, D. Richardson, T. L. Groy, *Acc. Chem. Res.* **1998**, *31*, 474−484.

[3] B. Moulton, M. J. Zaworotko, *Chem. Rev.* **2001**, *101*, 1629−1658.

[4] Y. B. Dong, M. D. Smith, R. C. Layland, H. C. zur Loye, *Chem. Mat.* **2000**, *12*, 1156−1161; R. Kitaura, K. Fujimoto, S. Noro, M. Kondo, S. Kitagawa, *Angew. Chem. Int. Ed.* **2002**, *41*, 133−135; H. Li, M. Eddaoudi, M. O′Keeffe, O. M. Yaghi, *Nature* **1999**, *402*, 276−279.

[5] O. M. Yaghi, G. M. Li, H. L. Li, *Nature* **1995**, *378*, 703−706.

[6] J. S. Seo, D. Whang, H. Lee, S. I. Jun, J. Oh, Y. J. Jeon, K. Kim, *Nature* **2000**, *404*, 982−986; S. S. Y. Chui, S. M. F. Lo, J. P. H. Charmant, A. G. Orpen, I. D. Williams, *Science* **1999**, *283*, 1148−1150.

[7] R. Kitaura, K. Seki, G. Akiyama, S. Kitagawa, *Angew. Chem. Int. Ed.* **2003**, *42*, 428−431.

[8] O. M. Yaghi, H. L. Li, T. L. Groy, *J. Am. Chem. Soc.* **1996**, *118*, 9096−9101; T. L. Hennigar, D. C. MacQuarrie, P. Losier, R. D. Rogers, M. J. Zaworotko, *Angew. Chem. Int. Ed. Engl.* **1997**, *36*, 972−973.

[9] M. L. Tong, J. X. Shi, X. M. Chen, *New J. Chem.* **2002**, *26*, 814−816; H. F. Zhu, W. Zhao, T. Okamura, B. L. Fei, W. Y. Sun, N. Ueyama, *New J. Chem.* **2002**, *26*, 1277−1279; B. L. Fei, W. Y. Sun, T. Okamura, W. X. Tang, N. Ueyama, *New J. Chem.* **2001**, *25*, 210−212; Z. Y. Fu, X. T. Wu, J. C. Dai, L. M. Wu, C. P. Cui, S. M. Hu, *Chem. Commun.* **2001**, 1856−1857.

[10] G. S. Papaefstathiou, R. Vicente, C. P. Raptopoulou, A. Terzis, A. Escuer, S. P. Perlepes, *Eur. J. Inorg. Chem.* **2002**, 2488−2493; S. Shova, G. Novitchi, M. Gdaniec, A. Caneschi, D. Gatteschi, L. Korobchenko, V. K. Voronkova, Y. A. Simonov, C. Turta, *Eur. J. Inorg. Chem.* **2002**, 3313−3318; T. Ezuhara, K. Endo, K. Matsuda, Y. Aoyama, *New J. Chem.* **2000**, *24*, 609−613.

[11] G. Yang, H. G. Zhu, B. H. Liang, X. M. Chen, *J. Chem. Soc., Dalton Trans.* **2001**, 580−585.

[12] Y. G. Li, H. Zhang, E. Wang, N. Hao, C. W. Hu, Y. Yan, D. Hall, *New J. Chem.* **2002**, *26*, 1619−1623.

[13] C. R. Kagan, D. B. Mitzi, C. D. Dimitrakopoulos, *Science* **1999**, *286*, 945−947.

[14] N. G. Pschirer, D. M. Ciurtin, M. D. Smith, U. H. F. Bunz, H. C. zur Loye, *Angew. Chem. Int. Ed.* **2002**, *41*, 583; C. J. Kepert, T. J. Prior, M. J. Rosseinsky, *J. Am. Chem. Soc.* **2000**, *122*, 5158−5168.

[15] O. Teichert, W. S. Sheldrick, *Z. Anorg. Allg. Chem.* **2000**, *626*, 1509−1513; M. Fujita, Y. J. Kwon, S. Washizu, K. Ogura, *J. Am. Chem. Soc.* **1994**, *116*, 1151−1152.

[16] F. A. A. Paz, J. Klinowski, *Chem. Commun.* **2003**, 1484−1485; F. A. A. Paz, A. D. Bond, Y. Z. Khimyak, J. Klinowski, *Acta Crystallogr. Sect. E.* **2002**, *58*, M730-M732; F. A. A. Paz, Y. Z. Khimyak, A. D. Bond, J. Rocha, J. Klinowski, *Eur. J. Inorg. Chem.* **2002**, 2823−2828.

[17] F. A. A. Paz, A. D. Bond, Y. Z. Khimyak, J. Klinowski, *Acta Crystallogr., Sect. C* **2002**, *58*, M608−M610.

[18] F. A. A. Paz, J. Klinowski, *J. Phys. Org. Chem.* **2003**, *16*, 772−782.

[19] D. C. Crans, F. L. Jiang, O. P. Anderson, S. M. Miller, *Inorg. Chem.* **1998**, *37*, 6645−6655.

[20] J. G. Mao, A. Clearfield, *Inorg. Chem.* **2002**, *41*, 2319−2324.

[21] A. Clearfield, C. V. K. Sharma, B. P. Zhang, *Chem. Mater.*

2001, *13*, 3099−3112; B. Zhang, D. M. Poojary, A. Clearfield, G. Peng, *Chem. Mater.* **1996**, *8*, 1333−1340; D. M. Poojary, B. Zhang, A. Clearfield, *Angew. Chem. Int. Ed. Engl.* **1994**, *33*, 2324−2326.

[22] S. O. H. Gutschke, D. J. Price, A. K. Powell, P. T. Wood, *Angew. Chem. Int. Ed.* **1999**, *38*, 1088−1090.

[23] J. G. Mao, Z. K. Wang, A. Clearfield, *Inorg. Chem.* **2002**, *41*, 6106−6111.

[24] S. Boudin, A. Guesdon, A. Leclaire, M. M. Borel, *Int. J. Inorg. Mater.* **2000**, *2*, 561−579.

[25] J. M. Shi, J. Q. Xu, W. T. Yu, L. D. Liu, C. J. Wu, *Pol. J. Chem.* **2001**, *75*, 1695−1701; M. H. Lee, N. H. Heo, S. Hayashi, *Polyhedron* **1998**, *17*, 55−62; C. Djordjevic, P. L. Wilkins, E. Sinn, R. J. Butcher, *Inorg. Chim. Acta* **1995**, *230*, 241−244; Y. G. Wei, S. W. Zhang, G. Q. Huang, M. C. Shao, *Polyhedron* **1994**, *13*, 1587−1591; A. E. Lapshin, Y. I. Smolin, Y. F. Shepelev, M. Sivak, D. Gyepesova, *Acta Crystallogr. Sect. C* **1993**, *49*, 867−870; L. Kuchta, M. Sivak, F. Pavelcik, *J. Chem. Res. (S)* **1993**, 393−393; K. Okamoto, J. Hidaka, M. Fukagawa, K. Kanamori, *Acta Crystallogr. Sect. C* **1992**, *48*, 1025−1027.

[26] K. Kanamori, K. Ishida, K. Fujimoto, T. Kuwai, K. Okamoto, *Bull. Chem. Soc. Jpn.* **2001**, *74*, 2377−2378; B. J. Hamstra, A. L. P. Houseman, G. J. Colpas, J. W. Kampf, R. LoBrutto, W. D. Frasch, V. L. Pecoraro, *Inorg. Chem.* **1997**, *36*, 4866−4874; M. MahroofTahir, A. D. Keramidas, R. B. Goldfarb, O. P. Anderson, M. M. Miller, D. C. Crans, *Inorg. Chem.* **1997**, *36*, 1657−1668; G. J. Colpas, B. J. Hamstra, J. W. Kampf, V. L. Pecoraro, *J. Am. Chem. Soc.* **1994**, *116*, 3627−3628.

[27] G. J. Colpas, B. J. Hamstra, J. W. Kampf, V. L. Pecoraro, *J. Am. Chem. Soc.* **1996**, *118*, 3469−3478; M. Sivak, J. Tyrselova, F. Pavelcik, J. Marek, *Polyhedron* **1996**, *15*, 1057−1062.

[28] L. Kuchta, M. Sivak, J. Marek, F. Pavelcik, M. Casny, *New J. Chem.* **1999**, *23*, 43−46; M. Sivak, V. Sucha, L. Kuchta, J. Marek, *Polyhedron* **1999**, *18*, 93−99.

[29] A. Kojima, K. Okazaki, S. Ooi, K. Saito, *Inorg. Chem.* **1983**, *22*, 1168−1174.

[30] Y. H. Chen, Q. T. Liu, Y. H. Deng, H. P. Zhu, C. N. Chen, H. J. Fan, D. Z. Liao, E. Q. Gao, *Inorg. Chem.* **2001**, *40*, 3725−3733; W. Plass, *Eur. J. Inorg. Chem.* **1998**, 799−805; D. C. Crans, H. J. Chen, O. P. Anderson, M. M. Miller, *J. Am. Chem. Soc.* **1993**, *115*, 6769−6776; S. Kitagawa, M. Munakata, M. Ueda, *Inorg. Chim. Acta* **1989**, *164*, 49−53; K. Wieghardt, M. Kleineboymann, W. Swiridoff, B. Nuber, J. Weiss, *J. Chem. Soc., Dalton Trans.* **1985**, 2493−2597.

[31] A. F. Wells, *Structural Inorganic Chemistry*, 4th ed., Clarendon Oxford University Press, **1975**.

[32] A. L. Spek, *Acta Crystallogr., Sect. A* **1990**, *46*, C34.

[33] G. B. Deacon, R. J. Phillips, *Coord. Chem. Rev.* **1980**, *33*, 227−250; C. Oldham, *Comprehensive Coordination Chemistry*, vol. 2, 1st ed. (Ed.: S. G. Wilkinson), Pergamon Press, **1987**, pp. 435−459.

[34] T. Kottke, D. Stalke, *J. Appl. Crystallogr.* **1993**, *26*, 615−619.

[35] Collect: Data Collection Software, R. Hooft, Nonius B. V., Delft, The Netherlands, **1998**.

[36] Z. Otwinowski, W. Minor, *Methods in Enzymology*, vol. 276, *Macromolecular Crystallography, Part A* (Eds.: C. W. Carter Jr., R. M. Sweet), Academic Press, New York, **1997**, p. 307.

[37] R. H. Blessing, *Acta Crystallogr., Sect. A* **1995**, *51*, 33−38; R. H. Blessing, *J. Appl. Crystallogr.* **1997**, *30*, 421.

[38] G. M. Sheldrick, *SHELXS 97, Program for Crystal Structure Solution*, University of Göttingen, **1997**.

[39] G. M. Sheldrick, *SHELXL 97, Program for Crystal Structure Refinement*, University of Göttingen, **1997**.

Received January 5, 2004
Early View Article
Published Online May 5, 2004